

See discussions, stats, and author profiles for this publication at: <https://www.researchgate.net/publication/228068531>

# Controlling the Morphology of Methylsilsesquioxane Monoliths Using a Two-Step Processing Method

ARTICLE *in* CHEMISTRY OF MATERIALS · OCTOBER 2005

Impact Factor: 8.35 · DOI: 10.1021/cm051900n

---

CITATIONS

23

---

READS

28

2 AUTHORS, INCLUDING:



**Hanjiang Dong**

Restek Corporation

15 PUBLICATIONS 263 CITATIONS

SEE PROFILE

# Controlling the Morphology of Methylsilsesquioxane Monoliths Using a Two-Step Processing Method

Hanjiang Dong and John D. Brennan\*

Department of Chemistry, McMaster University, Hamilton, Ontario, L8S 4M1, Canada

Received August 23, 2005. Revised Manuscript Received November 13, 2005

A new method for fabricating methylsilsesquioxane (MSQ) materials with similar chemical composition yet easily tailored pore morphology is described. MSQ materials were formed using an acid/base two-step processing method (B2). By varying the duration of the initial acidic step, it is possible to control the size and distribution of the clusters resulting from the polymerization of methytrimethoxysilane, which affect the gelation and phase separation time in the second basic step. As a result, the microstructure of the resultant MSQ monoliths, including pore volume, pore size, and distribution of meso- and macropores, can be varied over a wide range. The origin of this phenomenon is discussed based on the sol–gel polymerization kinetics and growth models for MSQ materials. Macroporous materials show minimal shrinkage, allowing for the fabrication of monolithic columns in a 100  $\mu\text{m}$  fused silica capillary with no pullaway, and indicating the potential of this highly stable material as a new chromatographic stationary phase.

## Introduction

Sol–gel processing<sup>1</sup> has attracted considerable interest owing to the ability to use this method to design monolithic materials with well-controlled meso-<sup>2</sup> or macroporous<sup>3,4</sup> morphologies. Macroporous structures, which are usually formed by either templating<sup>3</sup> or spinodal decomposition,<sup>4</sup> can provide enhanced mass transport, which is extremely important for the development of solid-phase catalysts, membranes, adsorbents, chromatographic stationary phases,<sup>5</sup> and protein supports.<sup>6</sup> In addition, large pores reduce the capillary force during drying and increase gel permeability, allowing fabrication of materials that undergo minimal shrinkage and cracking upon aging.<sup>1</sup> However, in cases where templates are used, the need to remove the template, usually by calcination, can lead to up to 50% shrinkage by volume.<sup>3b,4</sup>

Recently, several groups have reported on the formation of macroporous monolithic methylsilsesquioxane (MSQ) materials by polycondensation of methyltrimethoxysilane (MTMS)<sup>7</sup> and methyltriethoxysilane precursors.<sup>8</sup> Interest in such materials stems from their potential use as superhy-

drophobic materials<sup>9</sup> and monolithic chromatography columns.<sup>7</sup> Such materials can be formed with a relatively wide range of morphologies without the need for polymer additives, owing to their inherent ability to undergo self-induced phase separation as a result of immiscibility between the growing MSQ chains and the supporting solvent.<sup>7,8</sup> These materials also show less cracking and improved stability to extreme pH values than conventional macroporous silica materials,<sup>10</sup> making them of potential use for the development of a new generation of highly stable monolithic stationary phases.

Monolithic MSQ materials can be formed using either one-step processing methods at extreme pH values<sup>11</sup> or a recently reported two-step processing (B2) method under more mild conditions.<sup>10</sup> In general, the formation of monolithic gels using one-step processing is difficult owing to the tendency for the material to undergo macroscopic phase separation instead of gelation. With use of this method, monolithic gels can be obtained only with high concentrations of the monomer and/or under highly acidic or basic conditions.<sup>10,11</sup> Using the B2 method, it is possible to attain both rapid hydrolysis and condensation, which avoids macroscopic phase separation during MTMS polymerization. A key aspect of the B2 method is that it allows for separation of the hydrolysis and condensation steps in the processing of MSQ materials, which provides control over the MSQ morphology by adjustment of processing parameters such as the concentration of catalyst used in the first and second steps and the water-to-MTMS molar ratio.<sup>10</sup> However, as described in this paper, using the B2 method also provides very fine control

\* To whom correspondence should be addressed. Tel: (905) 525-9140 (ext. 27033). Fax: (905) 527-9950. E-mail: brennanj@mcmaster.ca. Internet: <http://www.chemistry.mcmaster.ca/faculty/brennan>.

- (1) Brinker, C. J.; Scherer, G. W. *Sol–Gel Science The Physics and Chemistry of Sol–Gel Processing*; Academic Press: New York, 1990.
- (2) Kresge, C. T.; Leonowicz, M. E.; Roth, W. J.; Vartuli, J. C.; Beck, J. S. *Nature* **1992**, 359, 710.
- (3) (a) Velev, D. O.; Lenhoff, A. M. *Curr. Opin. Colloid Interface Sci.* **2000**, 5, 56. (b) Imhof, A.; Pine, D. J. *Adv. Mater.* **1998**, 10, 697.
- (4) Nakanishi, K. *J. Porous Mater.* **1997**, 4, 67.
- (5) Cabrera, K. J. *Sep. Sci.* **2004**, 27, 843.
- (6) (a) Hodgson, R. J.; Brook, M. A.; Brennan, J. D. *Anal. Chem.* **2005**, 77, 4404. (b) Hodgson, R. J.; Chen, Y.; Zhang, Z.; Tleugabulova, D.; Long, H.; Zhao, X.; Organ, M.; Brook, M. A.; Brennan, J. D. *Anal. Chem.* **2004**, 76, 2780.
- (7) Kanamori, K.; Yonezawa, H.; Nakanishi, K.; Hirao, K.; Jinnal, H. J. *Sep. Sci.* **2004**, 27, 874.
- (8) Wongcharee, K.; Brungs, M.; Chaplin, R.; Hong, Y. J.; Sizgek, E. J. *Sol-Gel Sci. Technol.* **2004**, 29, 115.

- (9) Shirtcliffe, N. J.; McHale, G.; Newton, M. I.; Perry, C. C. *Langmuir* **2003**, 19, 5626.
- (10) Dong, H.; Brook, M. A.; Brennan, J. D. *Chem. Mater.* **2005**, 17, 2807.
- (11) Loy, D. A.; Mather, B.; Straumanis, A. R.; Baugher, C.; Schneider, D. A.; Sanchez, A.; Shea, K. J. *Chem. Mater.* **2004**, 16, 2041.

over the morphologies of MSQ materials by adjusting a single parameter, the duration of the initial acid-catalyzed hydrolysis step, with all other parameters held constant. Thus, a range of different morphologies can be accessed using a single sample composition (i.e., constant pH, water-to-silicon ratio, solvent system, and temperature). From a processing point of view, this provides a facile route to optimize sample morphology with precise control over the size and distribution of macropores.

Herein, we describe how altering the duration of the initial acid-catalyzed hydrolysis step alters the morphology of bulk MSQ materials that are prepared using a specific composition consisting of a water:MTMS ratio ( $r$ ) of 3 and a methanol:MTMS ratio ( $R$ ) of 1.05. We note that other ratios could also lead to macroporous MSQ materials; however, the ratios chosen provide good reproducibility and sufficiently high silica density to allow fabrication of columns, while showing significant sensitivity to the duration of the acidic step. The changes in the phase separation and gelation time using different reaction times are examined and related to alterations in morphology as monitored using SEM, mercury, and nitrogen porosimetry. Changes in MSQ morphology are described in the context of the kinetic activity of silicon sites and kinetic growth models for MSQ materials in light of recently reported  $^{29}\text{Si}$  NMR data. The advantages of these materials for chromatographic applications are also described.

### Experimental Section

All chemicals, including methyltrimethoxysilane, ammonium hydroxide ( $\text{NH}_4\text{OH}$ ), hydrochloric acid ( $\text{HCl}$ ), and methanol ( $\text{MeOH}$ ) were of analytical grade or above and were purchased from Aldrich (Ontario, Canada). All reagents were used as received. All water was obtained from a Milli-Q Synthesis A10 water purification system. Fused-silica capillary was purchased from Polymicro (Arizona).

MSQ monoliths were prepared using 1 mL of MTMS + 0.3 mL of MeOH + 0.186 mL of 0.01 M  $\text{HCl}$  + 0.186 mL of 1 M  $\text{NH}_4\text{OH}$ . First, MTMS, MeOH, and 0.01 M  $\text{HCl}$  were mixed for a specified time ( $t_{\text{acid}}$ ) at room temperature (ca. 20 °C) to promote hydrolysis and early stage condensation reactions, after which 1 M  $\text{NH}_4\text{OH}$  was added to the solution to accelerate condensation reactions. Gelation time and phase separation time were taken from the point where 1 M  $\text{NH}_4\text{OH}$  was added. After gelation, MSQ monoliths were aged at room temperature for 1 day and at 40 °C for 1 day. MSQ gels were dried at 120 °C for 1 day and/or at 300 °C for 1 day for characterization by SEM or porosimetry, respectively.

The conditions used to prepare MSQ columns and bulk samples were similar except that columns were fabricated using 0.02 M  $\text{HCl}$  in the initial acid hydrolysis step and the duration of the acidic step was 3 h 40 min. About 10 min after the base was added, the MSQ sol was pushed into the capillary by hand using a 3 mL syringe. After gelation and phase separation, the column was aged at room temperature for 2 days and at 70 °C for 2 h. Subsequently, the column was dried at 120 °C for 2 h and at 300 °C for 1 day.

Porosity measurements were performed by mercury porosimetry using a Quantachrome Poremaster GT and nitrogen sorption porosimetry using a Quantachrome Nova 2000. All samples were degassed at 300 °C for at least 10 h before measurement. An equilibration time of 4 min was used for each point during adsorption and desorption of nitrogen. The specific surface area (7

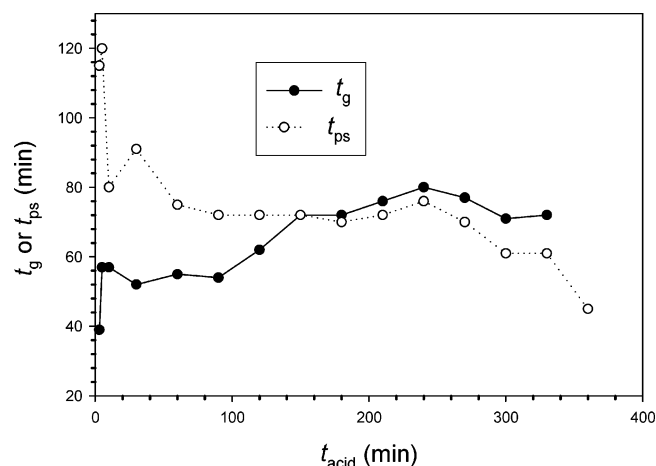


**Figure 1.** Effect of the duration of the acidic step ( $t_{\text{acid}}$ ) on gelation time ( $t_g$ ) and phase separation time ( $t_{ps}$ ) during MTMS polymerization.

points,  $0.05 < p/p_0 < 0.30$ ) and pore size distribution were calculated using the multipoint BET equation and BJH (Barrett, Joyner, and Halenda) model, respectively. The total pore volume was estimated at a pressure close to  $p/p_0 = 1$ . Images of gels were obtained using a Philips 515 scanning electron microscope (SEM) at an operating voltage of 20 kV. The surfaces were previously sputter-coated with gold to avoid charging effects during observation.

### Results and Discussion

Figure 1 shows the effect of the duration of the acidic step ( $t_{\text{acid}}$ ) on gelation and phase separation times. Both the gelation time ( $t_g$ ) and phase separation time ( $t_{ps}$ ) are key parameters that control the final morphology of sol–gel-derived materials. The terms “gelation time” and “phase separation time” refer to the times for the reaction mixture to lose flow and to undergo microscale phase separation, as evidenced by the appearance of opaqueness, respectively. Both values are measured from the time when the base is added. As shown in Figure 1, increasing the duration of the acidic step leads to an increase in  $t_g$  and a decrease in  $t_{ps}$ , leading to an increase in  $t_g - t_{ps}$ . When using very short  $t_{\text{acid}}$  values, the gelation time is shorter than the phase separation time. The crossover point where  $t_{ps}$  becomes less than  $t_g$  is at  $t_{\text{acid}} = 2.5$  h; beyond this point phase separation always occurs prior to gelation. It is noteworthy that gelation and phase separation both occur over a wide range of  $t_{\text{acid}}$  values. Thus, under the conditions employed, a wide range of  $t_g - t_{ps}$  values can be accessed by simply varying the duration of the acidic step. This has clear implications in the control of morphology, as the difference in gelation and phase separation times controls the feature sizes within the resulting materials.<sup>4</sup>

At very long  $t_{\text{acid}}$  times ( $> 6$  h) gelation no longer occurs; instead, macroscopic phase separation (flocculation) occurs, resulting in a two-phase resin, and thus a self-supporting monolith is not formed. It should be pointed out that macroscopic two-phase resins are different from the precipitates that are obtained under weakly acidic conditions. Precipitates result from fully condensed oligomers due to the extensive cyclization during MTMS polymerization in the presence of acid. We did not observe any precipitate in

our samples before the addition of base and it is well-established that cyclization is suppressed under basic conditions. On the other hand, two-phase resins are highly cross-linked polymers that can form in the presence of base.<sup>10</sup>

It is interesting that for MSQ materials it is possible to have phase separation occur after gelation of the material. This situation generally does not hold for silica materials derived from TEOS or TMOS in their parent solvents EtOH or MeOH, where the formation of the silica gel prevents spinodal decomposition (microscopic phase separation). In the case of MSQ, the lower overall degree of cross-linking owing to the presence of the methyl group causes the gel network of MSQ to be more flexible. As the degree of condensation increases, the polymerized MSQ species become immiscible with the highly polar solvents due to the intrinsic hydrophobicity of Si-CH<sub>3</sub> groups. As the polymer reaction continues, the flexible gel network is prone to collapse to exclude occluded solvent, resulting in the formation of coarse domains even after gelation. A similar phenomenon was previously reported in a specially designed acid-catalyzed TMOS-formamide (FA)-water system, in which highly polar FA was used to decrease the miscibility between solvents (water and MeOH) and silica oligomers and a low concentration of water (molar ratio of TMOS/water < 2) was added to reduce the cross-linking density in the gel network.<sup>12</sup> As a result, visible phase separation after gelation in the sol-gel system is due to the immiscibility between oligomers or polymer clusters and solvents, and the overall low degree of cross-linking in the gelled system.

It is useful to compare the gelation behavior for MSQ materials using different  $t_{\text{acid}}$  values to that obtained for TEOS. Boonstra and Bernards used a B2 method to form silica materials from TEOS and examined the effect of  $t_{\text{acid}}$  on  $t_g$ . (Note: these materials did not phase separate; thus, no  $t_{\text{ps}}$  values were obtained.)<sup>13</sup> For TEOS, the  $t_g$  values initially decreased as  $t_{\text{acid}}$  increased, mainly owing to the low levels of hydrolyzed monomer available for subsequent condensation reactions when using short  $t_{\text{acid}}$  times. Longer  $t_{\text{acid}}$  values lead to the accumulation of hydrolyzed species and decreased  $t_g$ . On the other hand,  $t_g$  in MTMS systems was shortest at  $t_{\text{acid}} = 1$  min (the shortest time at which we conducted the second step) and increased with  $t_{\text{acid}}$ . This indicates that hydrolysis of MTMS is not rate-limiting in the gelation reaction, even after a hydrolysis time of only 1 min. Thus, MTMS reaches hydrolysis pseudo-equilibrium within 1 min under our experimental conditions, consistent with the fact that hydrolysis of MTMS in the presence of an acid is very fast.<sup>14</sup> Other factors must then control the changes in gelation time (and phase separation time) with the increased duration of the acidic step.

The sol-gel chemistry of MTMS under both acidic and B2 conditions has been extensively investigated by <sup>29</sup>Si NMR.<sup>15</sup> When a short  $t_{\text{acid}}$  value (<2 h) is used, the MTMS

undergoes rapid hydrolysis and forms only monomers, dimers, low-order oligomers, and predominantly linear oligomers. Cyclic species do not form under acidic conditions and monomers are still present after a reaction time of 1.5 h in a similar system with a molar ratio of MTMS:MeOH:H<sub>2</sub>O (in 0.01 M HCl). Thus, systems with short  $t_{\text{acid}}$  values can be regarded as reactions occurring under one-step basic conditions without the limitation of slow hydrolysis because the sizes of the resultant oligomers will remain small. Under basic conditions, condensation kinetics control  $t_g$  (and  $t_{\text{ps}}$ ), and the key requirement to undergo polymerization is to have monomers (or small oligomers) join onto growing clusters (reaction-limited monomer-cluster growth), which is the typical mechanism of base-catalyzed formation of MSQ materials.<sup>16</sup> When transferred to basic conditions, clusters that initially form will grow rapidly, leading to a broad cluster distribution. The largest clusters will eventually grow to spanning clusters, resulting in gelation. Under such conditions, the degree of condensation at the gel point is expected to be low. Entropic factors based on the low cross-link density and enthalpic factors related to the high concentrations of residual groups make the MSQ oligomers miscible with the solvents, and thus phase separation is delayed.

Condensation under acidic conditions is much slower and decreases with connectivity around the silicon center.<sup>17</sup> Thus, as  $t_{\text{acid}}$  increases, the initially hydrolyzed monomers will grow to form longer, predominantly linear oligomers owing to the higher reactivity of T<sup>1</sup> silicon sites (end species) relative to T<sup>2</sup> silicon sites (the sum of linear and cyclic species). Another distinct feature of MTMS polycondensation, like other silicon alkoxides, is that linear species gradually change into cyclic species mainly through the intramolecular reaction of a tetramer as  $t_{\text{acid}}$  increases. However, these cyclic species are not stable in the presence of base because <sup>29</sup>Si NMR shows a drastic decrease in the amount of cyclic and polycyclic species under B2 or single-step basic conditions compared to the result under acidic conditions. This conclusion was also supported by IR analysis. Nevertheless, the transformation of linear to cyclic four-membered silicon rings does support the assumption that the distribution of cluster sizes in the presence of acid is relatively small. Under such conditions, the maximum ratio of intermediate silicon sites T<sup>1</sup> and T<sup>2</sup> relative to the total silicon concentration is around 0.7,<sup>14a</sup> which is much higher than the value of 0.45 predicted by the random reaction model.<sup>18</sup> Indeed, no branched or polycyclic species were observed in a similar system until a reaction time of 5 h. The limited condensation among condensed silicon sites will produce MSQ oligomers with small sizes and narrow cluster size distributions. As  $t_{\text{acid}}$  increases, the number and size of these clusters increases, but the distribution of cluster sizes will be much narrower than in the case where the clusters form under basic conditions. Upon the addition of base, the condensation reaction can no longer proceed under monomer-cluster growth conditions owing to the low level of monomer and

(12) Kaji, H.; Nakanishi, K.; Soga, N. *J. Non-Cryst. Solids* **1995**, *185*, 18.

(13) Boonstra, A. H.; Bernards, T. N. M. *J. Non-Cryst. Solids* **1988**, *105*, 207.

(14) (a) Dong, H.; Lee, M.-H.; Thomas, R. D.; Zhang, Z.; Reidy, R. F.; Mueller, D. W. *J. Sol-Gel Sci. Technol.* **2003**, *28*, 5. (b) Alam, T. M.; Assink, R. A.; Loy, D. A. *Chem. Mater.* **1996**, *8*, 2367.

(15) Dong, H. Ph.D. Thesis, University of North Texas, 2003.

(16) Schaefer, D. W. *MRS Bull.* **1994**, *19*, 49 and references therein.

(17) Sanchez, J.; Rankin, S. E.; McCormick, A. V. *Ind. Eng. Chem. Res.* **1996**, *35*, 117.

(18) Devereux, F.; Boilot, J. P.; Chaput, F. *Phys. Rev. A* **1990**, *41*, 6901.



short oligomers present. The polymerization reaction after shifting to basic conditions must then follow the reaction-limited cluster-cluster aggregation model.<sup>16</sup> As this process is expected to be inherently slower than the monomer-cluster growth process, the gelation time will be delayed owing to the difficulty in forming spanning clusters. On the other hand, the narrower size distribution for the clusters will lead to poorer miscibility, which will decrease as the initial cluster size grows (and hence as  $t_{\text{acid}}$  increases). In addition, the resultant clusters of the first step in these B2 systems apparently hinder the occurrence of the spanning cluster to form a gel and result in a high degree of condensation at the gel point. However, the point of phase separation is less affected because it depends on the entropy of mixing and the degree of condensation of all the clusters, not just the spanning cluster. Thus, as  $t_{\text{acid}}$  increases, one should expect an increase in  $t_g$  and a decrease in  $t_{\text{ps}}$ , as observed.

An important point to note is that the  $t_g$  value increases and the  $t_{\text{ps}}$  value drops most dramatically at very short  $t_{\text{acid}}$  values ( $t_{\text{acid}} = 5$  min). This suggests that the initial growth of clusters is relatively fast under the conditions employed in our study. The further increase in  $t_g$  over the range of  $t_{\text{acid}}$  values from 100 to 200 min values may reflect a loss of the remaining linear oligomers that may be present for relatively long times under acidic conditions. This would suggest that  $t_{\text{acid}} = 100$  min may represent the point where the cluster-cluster mechanism of growth begins to take over from the oligomer-cluster model upon shifting to basic conditions.

SEM images, shown in Figure 2, indicate that the feature sizes (pore and particle diameters) of MSQ gels increase with the increase of  $t_g - t_{\text{ps}}$ . These data show that, in cases where gelation occurs prior to phase separation (panel A), materials that contain primarily mesopores are formed. However, systems in which the gelation time is only slightly longer than the phase separation time (4–10 min, panels B and C) show a significant fraction of macropores, with the size of macropores increasing with the increase in  $t_g - t_{\text{ps}}$ . Systems that have very long hydrolysis times, and correspondingly large differences in gelation and phase separation time (panel D), do not form self-supporting monoliths, but rather form flocculated materials that show very large feature sizes. The ability to control the value of  $t_g - t_{\text{ps}}$  by adjustment of the duration of the acidic step provides a means for very fine control over the feature sizes of the materials, leading to the ability to access a wide range of morphologies.

To demonstrate the utility of the low-shrinkage macroporous MSQ materials for fabrication of capillary-scale chromatographic columns, we also prepared a MSQ monolith in a 100  $\mu\text{m}$  capillary. SEM images of the monolithic column are shown in Figure 2E,F. The experimental conditions to prepare columns were slightly different from those used to make bulk samples. In this case, we used 0.02 M HCl in the first step and  $t_{\text{acid}}$  was 3.5 h. The difference in  $t_g - t_{\text{ps}}$  was 7 min. As expected, increasing the concentration of HCl enhanced hydrolysis and condensation, resulting in shorter  $t_{\text{acid}}$  values to achieve a similar degree of phase separation. It is clear that MSQ shows no radial shrinkage in the 100  $\mu\text{m}$  capillary. Indeed, even in bulk samples the linear

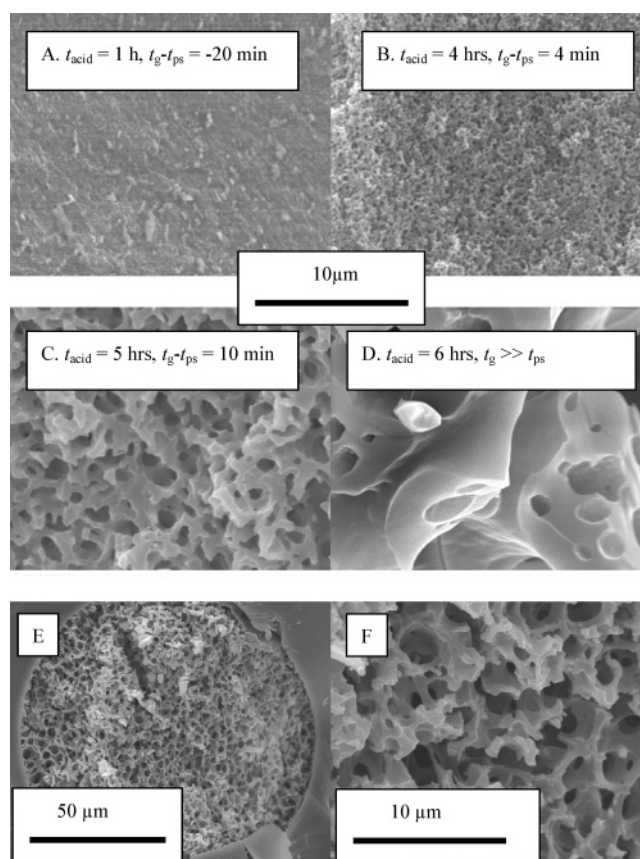


**Figure 2.** SEM images of MSQ monoliths formed using (A–D) different durations of the acidic step, after drying at 120 °C and (E, F) of a 100  $\mu\text{m}$  column containing monolithic MSQ.

shrinkage was less than 10%, and thus the presence of macropores provides an effective means to lower the capillary stress in the monolithic samples. The performance of MSQ-based columns in chromatographic applications is under investigation and will be reported elsewhere.

Mercury intrusion porosimetry data, which provides information on the nature of the macropores and mesopores bigger than 3.5 nm in the MSQ materials, is shown in Figure 3. These data were obtained for samples that were heated to 300 °C to densify the material and minimize pore size artifacts due to compression of materials under the high pressures used for the mercury intrusion experiment. The data show that the size and proportion of macropores increases as  $t_{\text{acid}}$  increases. When  $t_{\text{acid}} = 10$  min ( $t_g - t_{\text{ps}} = -33$  min) and  $t_{\text{acid}} = 1$  h ( $t_g - t_{\text{ps}} = -20$  min), the size of most pores is less than 50 nm and the pore size distribution is relatively broad, consistent with the formation of a mesoporous material. When  $t_{\text{acid}} = 2.5$  h,  $t_g$  is essentially equal to  $t_{\text{ps}}$  and the pore diameter is about 80 nm (becoming a predominately macroporous material) with a much narrower distribution than when  $t_{\text{acid}} = 10$  min and 1 h. This is consistent with there being a narrower distribution of cluster sizes at longer  $t_{\text{acid}}$  values, as described above. Surprisingly, at  $t_{\text{acid}} = 4$  h and  $t_g - t_{\text{ps}} = 4$  min, the material showed two peaks centered at 50 and 120 nm, respectively, leading once again to a broad pore size distribution. When  $t_{\text{acid}} = 5$  h and  $t_g - t_{\text{ps}} = 10$  min (identical to panel C in Figure 2), the material becomes macroporous with an average pore diameter of 1.6  $\mu\text{m}$  and has a very sharp pore size distribution.

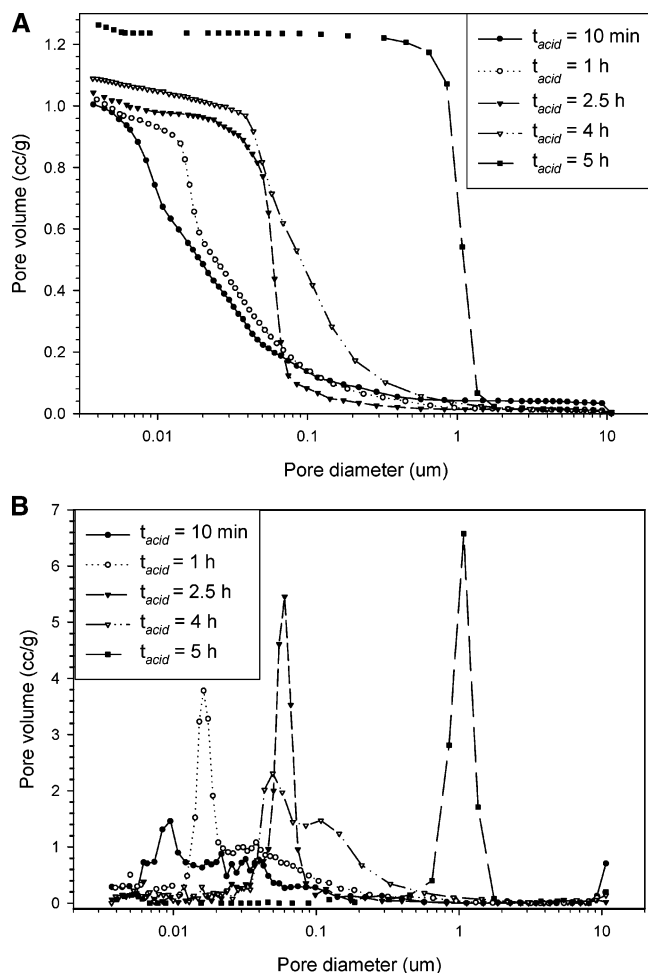


**Figure 3.** Cumulative (A) and differential (B) pore size distribution of MSQ gels formed using different durations of the acidic step after drying at 300 °C. The measurements were carried out by mercury porosimetry.

These results are in general agreement with the SEM data shown in Figure 2. While the total pore volumes accessible to mercury are similar from  $t_{\text{acid}}$  values of 10 min to 4 h, the pore volume at  $t_{\text{acid}} = 5$  h is notably higher. Because the shrinkage of these MSQ materials is the same, this may reflect the presence of high levels of small mesopores or micropores (pore diameter less than 3.5 nm) in samples prepared with shorter  $t_{\text{acid}}$  values. Those pores cannot be intruded by mercury, but can be probed by nitrogen sorption porosimetry.

Figure 4 shows the nitrogen adsorption–desorption isotherms (panel A) and BJH pore size distributions (panel B) of MSQ monoliths while Table 1 gives the associated surface areas, total pore volumes, and pore volumes for pores smaller than 3.5 nm in diameter. The errors in Table 1 are standard derivations, which are from three separately prepared samples examined on different days. Each sample was measured one or two times. A key characteristic of these isotherms is that the adsorption curve and desorption curve do not close at very low pressure. Increases in equilibration time and sample weight did not lead to closed isotherms. Analysis of standard alumina materials produced the expected isotherms, ruling out instrumental artifacts as the cause of this phenomenon. In addition, samples were degassed at 300 °C for at least 10 h prior to BET measurements. As a result, the low-pressure hysteresis is not likely the result of inadequate degassing.

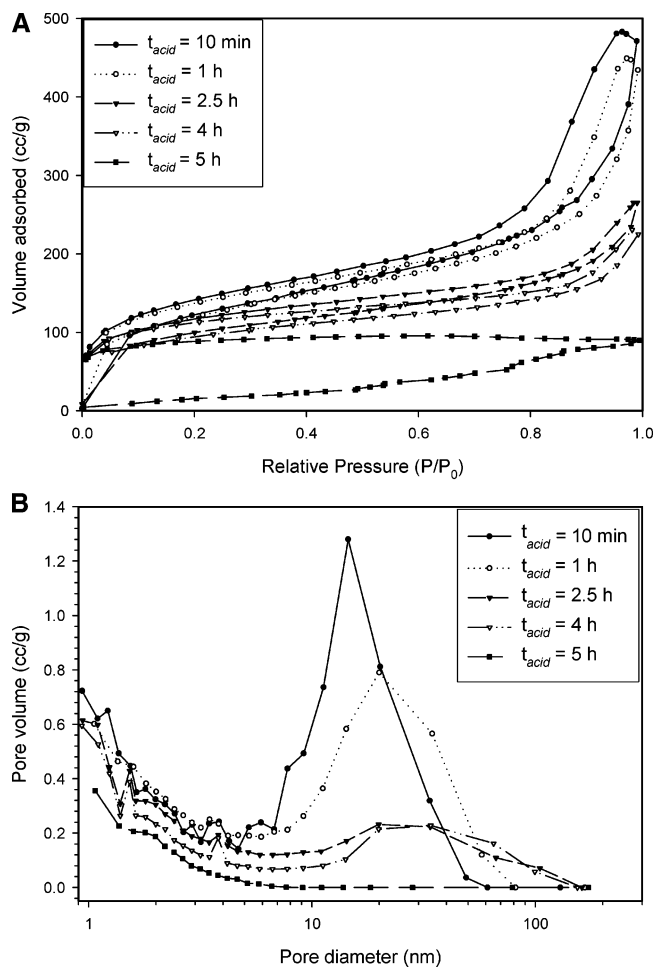


**Figure 4.** Nitrogen adsorption–desorption isotherms (A) and corresponding pore size distribution (B) of MSQ gels formed using different durations of the acidic step after drying at 300 °C.

Low-pressure hysteresis may be due to the swelling of the MSQ material during the adsorption process or to physical adsorption accompanied by chemisorption.<sup>19</sup> It is also possible that the low-pressure hysteresis results from the presence of micropores, as shown in Figure 4 panel B, which are expected to have relatively strong interactions with nitrogen. Our interpretation is supported by the nearly identical total pore volume of 1.3 cm<sup>3</sup>/g when one includes the pore volume from pores smaller than 3.5 nm (Table 1) and larger than 3.5 nm (Figure 3 panel A). This is also why the adsorption branch of all samples except that obtained at  $t_{\text{acid}} = 5$  h display a combination of type I (at low pressure) and IV (at high pressure) isotherms, which result from the presence of several different types of pores in the structure.

The pore size distribution obtained from nitrogen (Figure 4 panel B) and mercury (Figure 3 panel B) porosimetry results are in general agreement. For example, samples with a  $t_{\text{acid}}$  of 10 min and 1 h have a significant portion of mesopores (diameter between 2 and 50 nm and ~70%) with a pore volume ~0.7 cm<sup>3</sup>/g while those with  $t_{\text{acid}}$  values of 2.5 and 4 h have only a small fraction of pores in this range (<20%). On the other hand, there are almost no mesopores

(19) Sing, K. S. W.; Everett, D. H.; Hual, R. A. W.; Moscou, L.; Pierotti, R. A.; Rouquerol, J.; Siemieniowska, T. *Pure Appl. Chem.* **1985**, *57*, 603.

**Table 1. Surface Area, Total Pore Volume (PV), and Pore Volume from Pores with Diameters Less Than 3.5 nm for MSQ Monoliths Formed Using Different Durations of the Acidic Step ( $t_{\text{acid}}$ )**

$t_{\text{acid}}$ (h)	0.17	1	2.5	4	5
surface area (m <sup>2</sup> /g)	426.4 ± 10.5	418.2 ± 10.1	317.3 ± 7.9	296.5 ± 7.4	59.3 ± 11.5
total PV (cm <sup>3</sup> /g)	0.76 ± 0.10	0.68 ± 0.10	0.31 ± 0.07	0.29 ± 0.06	0.12 ± 0.04
PV < 3.5 nm (cm <sup>3</sup> /g)	0.242 ± 0.03	0.246 ± 0.03	0.195 ± 0.03	0.176 ± 0.02	0.108 ± 0.02

in the case where  $t_{\text{acid}} = 5$  h. Larger pore diameters correspond to a smaller surface area, and thus it is clear that variation of  $t_{\text{acid}}$  can be used to control surface area and pore volume (Table 1), which should be useful for optimizing both back pressure and capacity when such materials are used for chromatographic applications.

### Conclusions

A novel method using an acid/base two-step procedure to prepare macroporous methylsilsesquioxane (MSQ) monoliths with a narrow pore size distribution was discovered. Tight control over macropore size, varying from 50 nm to 1.6  $\mu\text{m}$  in diameter, was obtained by simply changing the duration of the acid step. Increasing the duration of acid step leads to an early onset of phase separation relative to gelation, result-

ing in an increase in pore size. The origin of this phenomenon is attributed to the size of the polymerized cluster in the acidic step, which affects the size distribution of clusters and occurrence of the spanning cluster in the basic step. MSQ gels showed no radial shrinkage in a 100  $\mu\text{m}$  fused silica capillary under optimized conditions, suggesting its potential application for the fabrication of monolithic columns. Elimination of templates and polymer additives is one of the major reasons that linear shrinkage of bulk MSQ gels during drying was only  $\sim 10\%$ . It is also noted that the entire sol-gel process (gelation, aging, and drying) could be performed under mild conditions (pH and temperature) upon addition of base in the second step, which may provide a route to immobilize and maintain the activity of lipophilic enzymes.

CM051900N